Journal of Mechanical Engineering Research and Developments
ISSN: 1024-1752
CODEN: JERDFO
Vol. 45, No. 3, pp. 80-97
Published Year 2022

Effects of Soret, Rotation, Hall, and Ion Slip on Unsteady MHD Flow of A Jeffrey Fluid Through A Porous Medium in The Presence of Heat Absorption and Chemical Reaction

Kodi Raghunath[†], Charankumar Ganteda[‡], Giulio Lorenzini[‡†]

[†]Department of Humanities and Sciences, Bheema Institute of Technology and Science, Adoni, Kurnool Dist, A.P, India, Pin-518301.

[‡]Department of Engineering Mathematics, College of Engineering, Koneru Lakshmaiah Education Foundation, Vaddeswaram, AP, India.

[‡†]Department of Engineering and Architecture, University of Parma, Parco Area delle Scienze 181/A, Parma 43124, Italy

*Corresponding Author Email: giulio.lorenzini@unipr.it

ABSTRACT

An unstable MHD free convection heat and mass transfer rotating flow of a viscous, incompressible, and electrically conducting fluid across an inclined porous plate embedded in a porous medium is studied to examine the Hall, ion slip, rotation, and Soret effects." It is assumed that the fluid is not Newtonian, specifically a Jeffrey fluid. In the presence of a first-order chemical reaction, the flow is directed through an infinitely moving an inclined plate that abruptly increases in temperature while flowing through a uniform porous medium in a spinning system. It is assumed that the liquid is opaque and absorbs and emits radiation in a manner that does not result in scattering. By using a two-term perturbation approach and placing physically suitable boundary conditions on the system, one may get an exact solution to the governing equations that describe the fluid's velocity, temperature, and concentration. It is also possible to derive the expressions for skin friction, the Nusselt number, and the Sherwood number. The numerical fluid velocity, temperature, and concentration values are presented graphically. In contrast, the numerical values of shear stress, rate of heat transfer, and rate of mass transfer across the plate are presented tabularly for various values of relevant flow parameters. The importance of shear stress, heat transfer rate, and mass transfer at the plate is presented for multiple values of pertinent flow parameters. This research is a state-of-the-art simulation tool that may optimize efficiency in design and operation within the fields of Naval Architecture, Offshore, and Marine Engineering, as well as within the Renewable Energy industry. In the limiting instance, the results are compared to what has been written.

KEYWORDS

Soret effect, second grade fluid, porous media, MHD, Hall and ion slip effects.

INTRODUCTION

The study of non-Newtonian fluids has garnered significant interest in various cutting-edge technological fields, including geothermal engineering, geophysical, astronomical, bio-fluid, and petroleum sectors. Many fundamental relations of non-Newtonian fluids have been studied due to the productive nature of the literature. The modern and designing applications of non-Newtonian fluids, such as the processing of paper, the production of plastics, the material industry, the handling of nourishment, wire, and edge covering, and the development of organic liquids, have given rise to the notion that non-Newtonian fluids are the domain of specialists. At low shear rates in narrow arteries, experiments show that blood may be modeled as a non-Newtonian fluid. This was found to be the case. Porous layers of biological tissue may represent a significant number of physiological systems. To adequately characterize the dynamics of these biofluids, several different non-Newtonian fluid models have been developed. One is the generalization of the Newtonian fluid known as the Jeffrey fluid. Bhatti

and Abbas [1] have discussed the influence of the magnetic field and wall slip condition on blood flow (Jeffrey model) in a non-uniform channel with peristalsis. Several researchers have studied Jeffrey fluid under various mechanical and thermal boundary conditions in the existing scientific literature. In a later study, the convective boundary layer flow of Casson fluid was investigated by Reddy [2] across an exponentially inclined porous stretched sheet with the effects of heat radiation and chemical reaction. Krishna Murthy [3] has researched two-dimensional MHD steady free convective mass transfer. The motion of an electrically conducting Jeffrey fluid in a channel through a porous medium when there is both a heat source and a chemical reaction present is called a Couette flow.

The intuitive system of cilia motion with a magnetic field and slip for the Jeffrey fluid model in a symmetric channel has been investigated by Akbar et al. [4]. They used the long-wavelength and low Reynolds approximations. Sandeep and Sulochana [5] studied the behavior of Jeffrey, Maxwell, and Oldroyd-B nanofluids in terms of momentum and heat transfer. They moved the nanofluids across a stretched surface with a non-uniform heat source. Researchers Sandeep and colleagues [6] explored the stagnation point flow of MHD Jeffrey nanofluid across a stretched surface with heat and mass transfer in the presence of non-uniform heat sources or sinks and chemical reactions using similarity transformation. Sandeep [7] researched the heat transfer flow of magnetic nanofluid across a stretched surface with an aligned magnetic field in the presence of thermal radiation and a non-uniform heat source/sink. Samad and Mansur-Rahman [8] explored the interaction of thermal radiation with an unsteady MHD flow via a permeable plate immersed in a porous liquid. They did this by using a plate submerged in porous media. Singapatnam et al. [9] investigated the effects of radiation and mass exchange on natural convective MHD streams as they moved over an imprudently isothermal plate with dissipation.

Investigation of hydromagnetic natural convection flow in a rotating medium is of considerable importance due to its application in various fields of astrophysics, geophysics, and fluid engineering, such as the maintenance and secular variations in Earth's magnetic field due to motion of Earth's liquid core, the structure of the magnetic stars, the internal rotation rate of the Sun, turbo machines, solar and planetary dynamo problems, rotating drum separators for liquid metal MHD applications, and rotating drum separators for liquid Unsteady hydromagnetic natural convection flow through a moving plate in a rotating media has been researched by several researchers in recent years. Some examples of these investigations are those conducted by Kythe and Puri [10], Toki [11], Nanousis [12], and Singh et al. [13].

The study of heat and mass transport in combination with chemical reactions is of significant practical value to engineers and scientists because it occurs practically everywhere in various engineering and scientific disciplines. This makes it an area of study of significant value to engineers and scientists." This kind of flow can be used in a wide variety of industries, including just two examples: the chemical and power industries. The impacts of diffusion thermal, radiation absorption and chemical reaction on the MHD free convective heat and mass transfer flow of a nanofluid confined within a semi-infinite flat plate were examined by Prasad et al. [14]. An unstable Casson nanofluid flow was used by Samrat et al. [15] in their study on the influence of heat radiation on the flow. This flow was conducted on a stretched surface. The effects of chemical reactions on different flow geometries have been studied by Raghunath and colleagues [16–18] under the impact of thermal diffusion, chemical reaction, and a heat source. Their findings are presented here. Researchers Ramachandra and colleagues [19] explored the effects of Soret on the unsteady free convection flow of a viscous incompressible fluid through a porous medium with high porosity confined by a vertical infinite moving plate with high porosity.

The effects of heat radiation are never considered in any of these experiments. However, the impact of thermal radiation on hydromagnetic natural convection flow with heat and mass transfer plays an essential part in various industrial processes, including glass production, the design of fins, steel rolling, furnace design, casting, and levitation, amongst others. In addition, several technical processes take place at very high temperatures, meaning an understanding of radiative heat transfer is necessary for constructing the appropriate apparatus. Examples of such engineering domains include nuclear power plants, gas turbines, and the many different types of propulsion systems used for missiles, airplanes, satellites, and space vehicles. It is important to note that, in

contrast to the convection and conduction processes, the governing equations that consider the effects of thermal radiation become rather intricate. As a result, there are a lot of obstacles to overcome while solving such problems.

On the other hand, various suitable approximations have been provided to solve the governing equations with radiative heat transport. Studying the oscillatory magnetohydrodynamic flow of a grey, absorbing-emitting fluid with a non-scattering medium through a flat plate in the presence of radiation while assuming the Rosseland flux model was performed by Raptis and Massalas [20]. Chamkha [21] has explored the effects of thermal radiation and buoyancy on hydromagnetic flow over an accelerating permeable surface that included a heat source or sink. Cookey and colleagues [22] investigated viscous dissipation and radiation's effect on the unsteady MHD free convection flow that occurs behind an infinitely heated vertical plate in a porous medium with time-dependent suction. Researchers Suneetha and colleagues [23] investigated the influence of thermal radiation on unsteady hydromagnetic free convection flow via an impulsively begun vertical plate with varying surface temperature and concentration. Ogulu and Makinde [24] studied an unstable hydromagnetic free convection flow of a dissipative and radiative fluid through a vertical plate with constant heat flux. Considering the impacts of viscous dissipation, Mahmoud [25] examined the effect of heat radiation on an unstable MHD free convection flow that was moving over an infinite vertical porous plate.

Recently, Veera Krishna and Chamkha [26] investigated the Hall and ion slip effects on the MHD convective flow of elastico-viscous fluid through the porous medium between two rigidly rotating parallel plates with a time-varying sinusoidal pressure gradient. [26] " "Recently, Veera Krishna and Chamkha [26] investigated the Hall and ion slip effects on the MHD convective flow of elastico-viscous fluid. According to research by Veera Krishna [27], the Hall and ion slip effects on MHD free convective rotating flow confined by the semi-infinite vertical porous surface were observed. The MHD laminar flow of an elastic-viscous electrically conducting Walter's-B fluid was studied in Veera Krishna's [28] research paper. This flow may occur in a circular cylinder or a pipe. Heat and mass transfer on unsteady MHD oscillatory flow of second-grade fluid through a porous medium between two vertical plates, under the impact of varying heat source/sink and chemical reaction, was described by Veera Krishna et al. [29].

The current investigation focuses on analyzing the effects of Hall and ion slip, rotation, and the Soret effect on an unsteady MHD free convection rotating flow of a viscous, incompressible, electrically conducting Jeffrey fluid that flows past an impulsively moving vertical plate in a porous medium. The flow of the fluid is being studied in a rotating fashion. A general solution is produced by first transforming the governing equations into a set of normalized equations, then solving the equations analytically using the perturbation method and obtaining the answer. On the fluid velocity, temperature, and concentration distributions are plotted, and discussed the effects of various involved parameters, such as the magnetic field parameter, Schmidt number, Prandtl number, and Grashof number for heat transfer and mass transfer, chemical reaction, thermal radiation, Hall ion slip, rotation, and the Soret effect. The significance of the findings acquired from doing this research lies in the fact that they provide the criteria for verifying the accuracy of various numerical or empirical methodologies. In addition, the findings that were produced from this study have the potential to be used in fields such as fluid mechanics and heat transport.

FORMULATION AND SOLUTION OF THE PROBLEM

We considered the heat and mass transport on an unsteady two-dimensional MHD convective flow of a viscous laminar heat generating/absorbing second-grade fluid over a semi-infinite vertical moving porous plate embedded in a uniform porous medium and applied to a uniform transverse magnetic field. We do this while considering Hall and ion slip effects. The Cartesian coordinate system is selected in such a way that the x-axis remains parallel to the wall in the direction of upward movement, and the z-axis is positioned so that it is perpendicular to the x-axis. A magnetic field with strength of B_0 and a uniform intensity is moving in a direction that is perpendicular to the flow. In their initial, undisturbed states, the fluid and the plate are both rotating in a fixed orientation relative to the perpendicular to the plate at a constant angular velocity. At the surface, the temperature and concentration are subject to random fluctuations; this is true for both the fluid and the plate. The investigational challenge may be seen as a physical model, which can be found in Figure 1.

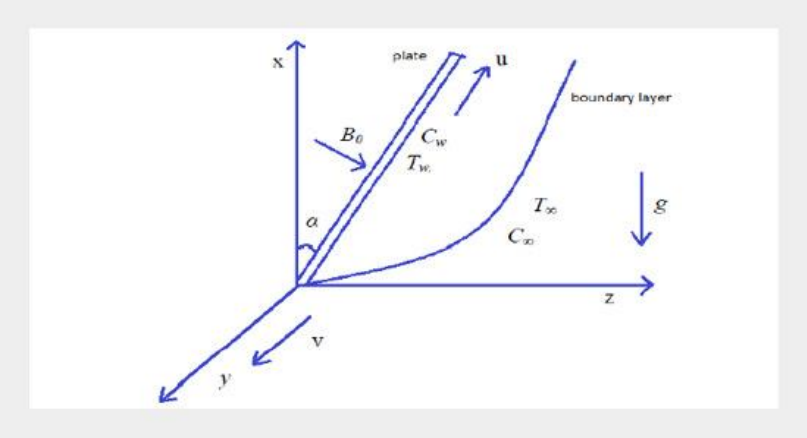

Figure 1. Physical sketch of the proposed model.

Under the Boussinesq approximation the flow of the fluid through the porous medium in a rotating channel is governed by the following equation:

$$\frac{\partial u}{\partial x}+\frac{\partial u}{\partial y}=0 \tag{1}$$

$$\frac{\partial u}{\partial t}+w\frac{\partial u}{\partial z}-2\Omega v=-\frac{1}{\rho}\frac{\partial p}{\partial x}+\mu\left(\frac{1}{1+\lambda}\right)\frac{\partial^2 u}{\partial z^2}+\frac{B_0 J_y}{\rho}-\frac{v}{k}u+g\beta(T-T_\infty^*)Cos\alpha+g\beta^*(C-C_\infty)Cos\alpha \tag{2}$$

$$\frac{\partial v}{\partial t}+w\frac{\partial v}{\partial z}+2\Omega u=-\frac{1}{\rho}\frac{\partial p}{\partial y}+\mu\left(\frac{1}{1+\lambda}\right)\frac{\partial^2 v}{\partial z^2}-\frac{B_0 J_x}{\rho}-\frac{v}{k}v \tag{3}$$

$$\frac{\partial T}{\partial t}+w\frac{\partial T}{\partial z}=\frac{k_1}{\rho C_p}\frac{\partial^2 T}{\partial z^2}-\frac{Q_0}{\rho C_p}(T-T_\infty)-\frac{1}{\rho C_p}\frac{\partial q_r}{\partial z} \tag{4}$$

$$\frac{\partial C}{\partial t}+w\frac{\partial C}{\partial z}=D\frac{\partial^2 C}{\partial z^2}+D_1\frac{\partial^2 T}{\partial z^2}-K_c(C-C_\infty) \tag{5}$$

Under the above assumptions, the appropriate boundary conditions for the distributions of velocity, temperature and concentration are given by:

$$u^*=U_0,\quad v=0, T=T_w+\varepsilon(T_w-T_\infty)e^{iwt}, C=C_w+\varepsilon(C_w-C_\infty)e^{iwt}\ \text{ at } z=0 \tag{6}$$

$$u\to U_\infty,\quad v\to 0,\quad T\to T_\infty \qquad C\to C_\infty \qquad \text{as} \quad z\to\infty \tag{7}$$

The equation of continuity yields that wis either a constant or some function of time, hence we assume that

$$w = - w^1_0 (1+ A\ \varepsilon\ e^{iwt}) \tag{8}$$

Where A is a real positive constant, ε and Aε are small less than unity, w_0 is the scale of the suction velocity which has a non-zero positive constant. We consider a mathematical model, for an optically thin limit gray gas near equilibrium in the form given by Cramer and Pai [30]. Later Grief et al. [31].

$$\frac{\partial q_r{}^*}{\partial y^*}=4\left(T^*-T_w^*\right)I \tag{9}$$

Where $I=\int_0^{\infty} K_{\lambda\omega}\left(\frac{\partial_{eb\lambda}}{\partial T}\right)_{\omega} d\lambda,$ $K_{\lambda\omega}$ the absorption coefficient at the wall and ebλ is Planck's function.

The electron-atom collision frequency is assumed to be very high, so that Hall and ion slip currents cannot be neglected. Hence, the Hall and ion slip currents give rise to the velocity in *y*-direction. When the strength of the magnetic field is very large, the generalized Ohm's law is modified to include the Hall and ion slip effect (Sutton and Sherman [32]).

$$J=\sigma\left(E+V\times B\right)-\frac{\omega_e\tau_e}{B_0}\left(J\times B\right)+\frac{\omega_e\tau_e\beta_i}{B_0^2}\left(\left(J\times B\right)\times B\right) \tag{10}$$

Further it is assumed that $\beta_e=\omega_e\tau_e \sim O(1)$ and $\beta_i=\omega_i\tau_i<<1,$ In the equation (10) the electron pressure gradient, the ion-slip and thermo-electric effects are neglected. We also assume that the electric field *E=0* under assumptions reduces to.

$$\begin{aligned}\left(1+\beta_i\beta_e\right)J_x+\beta_e J_y&=\sigma B_0 v\\ \left(1+\beta_i\beta_e\right)J_y+\beta_e J_x&=-\sigma B_0 v\end{aligned} \tag{11}$$

On solving above equations (11), we get

$$J_x=\sigma B_0\left(\alpha_2 u+\alpha_1 v\right) \tag{12}$$

$$J_y=-\sigma B_0\left(\alpha_2 v-\alpha_1 u\right) \tag{13}$$

$$Where\,\alpha_1=\frac{1+\beta_e\beta_i}{\left(1+\beta_e\beta_i\right)^2+\beta_e^2},\alpha_2=\frac{\beta_e}{\left(1+\beta_e\beta_i\right)^2+\beta_e^2}$$

Substituting the equations (12) and (13) in (2) and (3) respectively, the resulting equations are

$$\frac{\partial u}{\partial t}+w\frac{\partial u}{\partial z}-2\Omega v=-\frac{1}{\rho}\frac{\partial p}{\partial x}+\mu\left(\frac{1}{1+\lambda}\right)\frac{\partial^2 u}{\partial z^2}+\frac{\sigma B_0^2(\alpha_2 v-\alpha_1 u)}{\rho}-\frac{v}{k}u+g\beta(T-T_\infty^{**})Cos\alpha+g\beta^*(C-C_\infty)Cos\alpha \tag{14}$$

$$\frac{\partial v}{\partial t}+w\frac{\partial v}{\partial z}+2\Omega v=-\frac{1}{\rho}\frac{\partial p}{\partial y}+\mu\left(\frac{1}{1+\lambda}\right)\frac{\partial^2 v}{\partial z^2}-\frac{B_0^2\left(\alpha_2 u+\alpha_1 v\right)}{\rho}-\frac{v}{k}v \tag{15}$$

"Combining equations (2) and (3), let $q=u+iv$ and $\xi=x-iy$, we obtain"

$$\frac{\partial q}{\partial t}+w\frac{\partial q}{\partial z}+2i\Omega q=-\frac{1}{\rho}\frac{\partial p}{\partial \xi}+\mu\left(\frac{1}{1+\lambda}\right)\frac{\partial^2 q}{\partial z^2}+\frac{\sigma B_0^2(\alpha_2 v-\alpha_1 u)}{\rho}-\frac{v}{k}q+g\beta(T-T_\infty^{**})Cos\alpha+g\beta^*(C-C_\infty)Cos\alpha \tag{16}$$

Outside the boundary layer, Equation (16) gives

$$-\frac{1}{\rho}\frac{\partial p}{\partial \xi}=\frac{dU_\infty}{\partial t}+\frac{v}{k}U_\infty+\frac{\sigma B_0^2}{\rho}U_\infty \tag{17}$$

To normalize the mathematical model of the physical problem, we introduce the following non-dimensional quantities and parameters

$$q^* = \frac{q}{w_0}, w^* = \frac{w}{w_0}, z^* = \frac{w_0 z}{\nu}, U_0^* = \frac{U_0}{w_0}, U_\infty^* = \frac{U_\infty}{w_0}, t^* = \frac{t\, w_0^2}{\nu}, \theta = \frac{T - T_\infty}{T_w - T_\infty}, \phi = \frac{C - C_\infty}{C_w - C_\infty},$$
$$M^2 = \frac{\sigma B_0^2 \nu}{\rho w_0^2}, \Pr = \frac{\nu \rho C_p}{k_1} = \frac{\nu}{\alpha}, Sc = \frac{\nu}{D}, Gr = \frac{\nu g \beta (T_w - T_\infty)}{w_0^3}, Gm = \frac{\nu g \beta^* (C_w - C_\infty)}{w_0^3},$$
$$k = \frac{w_0^2 k}{\nu^2}, R = \frac{\Omega \nu}{w_0^2}, H = \frac{\nu Q_0}{\rho C_p w_0^2}, K_c = \frac{K_c \nu}{w_0^2}, F = \frac{4 I_1 \nu}{\rho C_p w_0^2}, So = \frac{D_1 (T_w - T_\infty)}{(C_w - C_\infty) w_0}, \quad (18)$$

Making use of non-dimensional variables the governing equations (2)-(5) reduces to

$$\frac{\partial q}{\partial t} - (1 + A\varepsilon e^{iwt}) \frac{\partial q}{\partial z} = \frac{dU_\infty}{dt} + \left(\frac{1}{1+\lambda}\right) \frac{\partial^2 q}{\partial z^2} - \gamma q + Gr\, \theta Cos\alpha + Gm\, \phi Cos\alpha \quad (19)$$

$$Where \gamma = M^2(\alpha_1 + i\alpha_2) + 2iR + \frac{1}{K}$$

$$\frac{\partial \theta}{\partial t} - (1 + A\varepsilon e^{iwt}) \frac{\partial \theta}{\partial z} = \frac{1}{\Pr} \frac{\partial^2 \theta}{\partial z^2} - (H + F)\theta \quad (20)$$

$$\frac{\partial \phi}{\partial t} - (1 + A\varepsilon e^{iwt}) \frac{\partial \phi}{\partial z} = \frac{1}{Sc} \frac{\partial^2 \phi}{\partial z^2} + So \frac{\partial^2 \theta}{\partial z^2} - K_c \phi \quad (21)$$

The corresponding boundary conditions are given by

$$q = U_0, \ \theta = 1 + \varepsilon e^{iwt}, \ \phi = 1 + \varepsilon e^{iwt} \qquad \text{at } z = 0 \quad (22)$$

$$q = 0, \ \theta = 0, \ \phi = 0 \qquad \text{as} \quad z \to \infty \quad (23)$$

Equation (19) and (21) represent a set of partial differential equations that cannot be solved in closed form however if can be reduced to a setoff ordinary differential equation in dimensionless form that can be solved analytically this can be done representing the velocity temperature and concentration as,

$$q = q_0(z) + \varepsilon e^{nt} q_1(z) + O(\varepsilon^2) \quad (24)$$

$$\theta = \theta_0(z) + \varepsilon e^{nt} \theta_1(z) + O(\varepsilon^2) \quad (25)$$

$$\phi = \phi_0(z) + \varepsilon e^{nt} \phi_1(z) + O(\varepsilon^2) \quad (26)$$

Substituting the equations (24), (25) and (26) into equation (19), (20) and (21),equating the harmonic and non-hamonic terms, the neglecting and higher order terms of $O(\varepsilon^2)$,one obtains the following pairs of equations (q_0, θ_0, ϕ_0) and (q_1, θ_1, ϕ_1).

$$\frac{\partial^2 q_0}{\partial z^2} + \frac{\partial q_0}{\partial z} - \gamma q_0 = -GrCos\alpha\, \theta_0 - Gm\, Cos\alpha\, \phi_0 \quad (27)$$

$$\frac{\partial^2 q_1}{\partial z^2} + \frac{\partial q_1}{\partial z} - \gamma q_1 = -Gr\, Cos\alpha\, \theta_1 - Gm\, Cos\alpha\, \phi_1 - A\frac{\partial q_0}{\partial z} + iwq_1 \quad (28)$$

$$\frac{\partial^2 \theta_0}{\partial z^2} + \Pr \frac{\partial \theta_0}{\partial z} - (H + F)\Pr \theta_0 = 0 \quad (29)$$

$$\frac{\partial^2\theta_1}{\partial z^2}+\Pr\frac{\partial\theta_1}{\partial z}-(iw+H+F)\Pr\theta_1=-\left(A\frac{\partial\theta_0}{\partial z}+Q_1\phi_1\right)\Pr \tag{30}$$

$$\frac{\partial^2\phi_0}{\partial z^2}+Sc\frac{\partial\phi}{\partial z}-Sc\,Kc\,\phi_0=-Sc\,So\frac{\partial^2\theta_1}{\partial z^2} \tag{31}$$

$$\frac{\partial^2\phi_1}{\partial z^2}+Sc\frac{\partial\phi_1}{\partial z}-(n+K_c)Sc\phi_1=\left(-A\frac{\partial\phi_0}{\partial z}-So\frac{\partial^2\theta_1}{\partial z^2}\right)Sc \tag{32}$$

The corresponding boundary conditions are:

$$q_0=U_0, q_1=0,\ \ \theta_0=1,\ \theta_1=1, \phi_0=1, \phi_1=1 \qquad \text{at } z=0 \tag{33}$$

$$q_0=0, q_1=0,\ \ \theta_0=0,\ \theta_1=0, \phi_0=0, \phi_1=0 \qquad \text{as} \quad z\to\infty \tag{34}$$

Solving equations (27) – (32) under the boundary conditions (33-34), the following solutions are obtained

$$\theta_0=\exp(-m_1z) \tag{35}$$

$$\theta_1=b_1\exp(-m_1z)+b_2\exp(-m_2z) \tag{36}$$

$$\phi_0=b_1\exp(-m_1z)+b_4\exp(-m_3z) \tag{37}$$

$$\phi_1=b_5\exp(-m_1z)+b_6\exp(-m_2z)+b_7\exp(-m_3z)+b_8\exp(-m_4z) \tag{38}$$

$$q_0=b_9\exp(-m_1z)+b_{10}\exp(-m_3z)+b_{11}\exp(-m_5z) \tag{39}$$

$$q_1=b_{12}\exp(-m_1z)+b_{13}\exp(-m_2z)+b_{14}\exp(-m_3z)+b_{15}\exp(-m_4z)+b_{16}\exp(-m_5z)+b_{17}\exp(-m_6z) \tag{40}$$

Substituting equations (35)–(40) in equation (24-26) we obtain the velocity temperature and concentration field:

$$q=b_9\exp(-m_1z)+b_{10}\exp(-m_3z)+b_{11}\exp(-m_5z)+\varepsilon e^{iwt}\begin{pmatrix}b_{12}\exp(-m_1z)+b_{13}\exp(-m_2z)+b_{14}\exp(-m_3z)+\\ b_{15}\exp(-m_4z)+b_{16}\exp(-m_5z)+b_{17}\exp(-m_6z)\end{pmatrix} \tag{41}$$

$$\theta=b_3\exp(-m_1z)+b_4\exp(-m_3z)+\varepsilon e^{iwt}(b_5\exp(-m_1z)+b_6\exp(-m_2z)+b_7\exp(-m_3z)+b_8\exp(-m_4z)) \tag{42}$$

$$\phi=\exp(-m_1z)+\varepsilon e^{iwt}(b_1\exp(-m_1z)+b_2\exp(-m_2z)) \tag{43}$$

"The skin friction:

$$\tau=\left(\frac{\partial q}{\partial z}\right)_{z=0}=-\left((b_9m_1+b_{10}m_3+b_{11}m_5)+\varepsilon e^{iwt}\begin{pmatrix}b_{12}m_1+b_{13}m_2+\\ b_{14}m_3+b_{15}m_4+b_{16}m_5+b_{17}m_6\end{pmatrix}\right) \tag{44}$$

Nusselt number:

$$Nu=-\left(\frac{\partial\theta}{\partial z}\right)_{z=0}=\left((m_1)+\varepsilon e^{iwt}(b_1m_1+b_2m_2)\right) \tag{45}$$

Sherwood number

$$Sh=-\left(\frac{\partial\phi}{\partial z}\right)_{z=0}=b_1m_1+b_4m_3+\varepsilon e^{iwt}(b_5m_1+b_6m_2+b_7m_3+b_8m_4) \tag{46}$$

RESULTS AND DISCUSSION

The objective of the present analysis is to study the effects of Soret, Hall and ion slip of unsteady free convective flow of a viscous incompressible electrically conducting fluid over an inclined porous plate under the influence of uniform transverse magnate field. The governing equations of the flow field are solved by a regular perturbation method for small Eckert number *Ec*. The closed form solutions for the velocity, temperature and concentration have been derived analytically and also its behavior is computationally discussed with reference to different flow parameters like Jeffrey parameter (λ), algle of inclination (α), Hartmann number (M), Hall parameter (β_e), ion slip parameter (β_e), the thermal Grashof number (Gr), the mass Grashof number (Gm), Permeability of porous media (K), Soret parameter (S_o), the Prandtl number (Pr), Chemical Reaction parameter (Kc), Schmidt number (Sc), Heat absorption parameter (H).

When the intensity of the magnetic field is increased, as shown in Fig. 2 we witness a reduction in the magnitude of the velocity components u and v and a reduction in the resultant velocity. Because the effects of a transverse magnetic field on an electrically conducting fluid produce a resistive type force (also known as the Lorentz force), which is similar to drag force, increasing M causes the drag force to increase, which causes the fluid's motion to slow down as a result of the increased drag force. Figure 3 illustrates that the succeeding velocity component u heightens v condenses as the permeability parameter K increases with time. When K is increased, the resultant velocity increases, increasing the thickness of the momentum boundary layer. Inside the flow zone that is occupied by the fluid, lower permeability results in a less noticeable increase in fluid speed. Figs. 4 and 5 show the influences of Hall current parameter (βe) and ion-slip parameter (βi) on the fluid velocity respectively. It can be seen from Figs. 4 and 5 that, the fluid velocity in the primary flow direction decreases in the boundary layer region in the vicinity of the plate while it increases in the boundary layer region away from the plate with increase in both Hall and ion-slip parameters. An increase in Hall current parameter give rise in the fluid velocity in the secondary flow direction everywhere in the boundary layer region except a thin region where it vanishes. It is true because Hall current is produced due to spiraling of conducting fluid particles about magnetic lines of force, whose tendency is to induce the secondary motion in the flow-field. The ion-slip current shows the reverse nature as that of Hall current on the fluid flow in the secondary flow direction.

The effects of thermal buoyancy force (Gr) and concentration buoyancy force (Gm) are depicted in Figs. 6 and 7. It is noticed that increase in both the thermal and mass Grashof numbers give rise in fluid velocity in the primary flow direction in the boundary layer region. This is due to the fact that increase in thermal and solutal Grashof numbers give rise in buoyancy effects and these induce more flow in the primary flow direction. Reverse flow arise in the secondary flow direction. On increasing the thermal and concentration Grashof numbers, the secondary velocity profiles increase in the boundary layer region away from the plate while decreases in the vicinity of the plate . It is also noted that in the absence of both thermal and concentration buoyancy forces there is no reversal flow in the secondary flow direction. It means that the buoyancy forces and the movement of the free-stream are responsible for induction of reversal flow.

Figure 8 display the influence of Soret number on primary and secondary fluid velocities. It is evident from Figure 8 that *u* and v increase on increasing Soret number *So*. This implies that Soret number tends to accelerate primary and secondary fluid velocities throughout the boundary layer region. Increasing Soret number indicates a fall in the viscosity of the mixture. This leads to increased inertia effects and diminished viscous effects. Consequently the velocity components increase, while the reversal behavior observed as Fig 9 in the case of Rotation parameter. Fig. 10-11 represents the effect of radiation parameter on velocity, and temperature respectively. From the figure it is noticed that an increase in radiation parameter reduces the primary velocity, where as it enhances for secondary velocity. Therefore, the resultant velocity is reduced with an increasing in R throughout the region occupied by the fluid. The effect of thermal radiation parameter is important in temperature profiles. It is observed that (Fig 11) the temperature decreases with the increasing of radiation parameter. It can also be seen that the thermal boundary layer decreases rapidly with the effect of radiation parameter."Figure 12 and 13 shows the effect of Jeffrey fluid parameter (λ) and angle of inclination (α)

on primary and secondary velocity respectively, It is evident that the primary velocity diminishes and secondary velocity enhances with increasing Jeffrey fluid and inclined parameters.

Figure 14 depicts the effect of Prandtl number (Pr) on temperature profiles in the presence of some selected fluids such as Hydrogen (Pr = 0.684), Air (Pr = 0.71), Carbon dioxide (Pr = 0.72) and Water (Pr = 1.0). This figure shows that an increase in the Prandtl number decreases the temperature of the flow field at all points. This is consistent with the thermal boundary layer thickness falling with increasing Prandtl number. In fig. 15 exhibited the disparities of temperature profiles with different values of Heat source Specification H, Increasing the heat source parameter reduces the temperature of the flow field. This may happen due to the elastic property of the fluid. It is noticed from figure16 that, the species concentration ϕ increases on increasing Soret number *So*. An increase in Soret effect indicates increasing molar mass diffusivity, as seen from definition of *So*. The surge in molecular mass diffusivity causes the concentration to rise. This implies that, Soret number tends to enhance the species concentration of the fluid. Figures 17-18 depict the effect of chemical reaction parameter Kc, and the Schmidt number, on concentration distribution. An improvement in the chemical reaction parameter is seen in Figure 17. Kc rapidly depleted the concentration profiles. The concentration domain shrinks because the chemical reaction effects on the amounts of solutal particles increase as chemically responding parameters increase. As a result, the chemical reaction narrows the solute boundary stratum width. In fig 18 expressed as the concentration distribution decreases at all points of the flow field with the increase in the Schmidt number Sc. This shows that the heavier diffusing species have a greater retarding effect on the concentration distribution of the flow field.

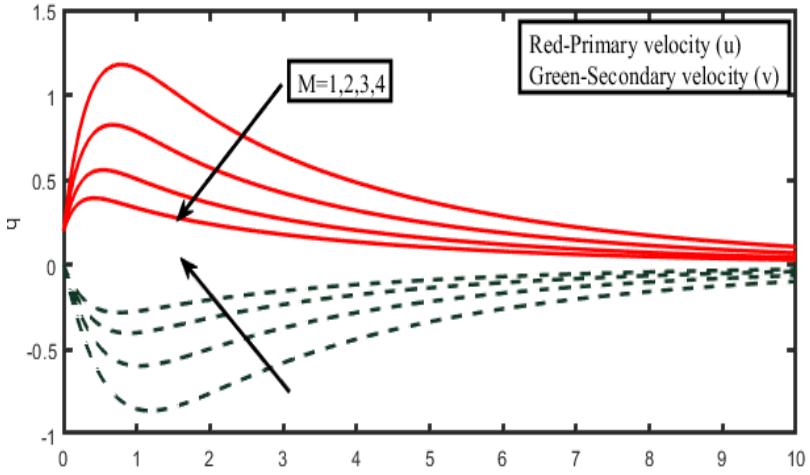

Figure 2. Velocity profiles for u and v for Magnetic field parameter (M)

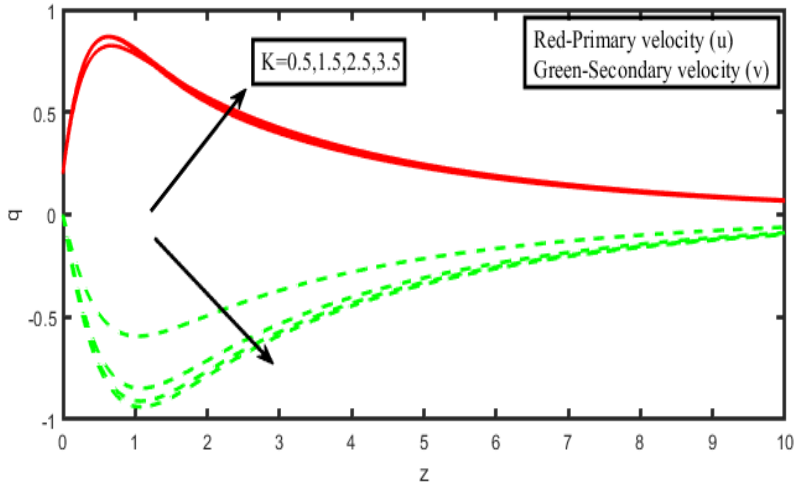

Figure 3. Velocity profiles for u and v for Permeability of porous media (K)

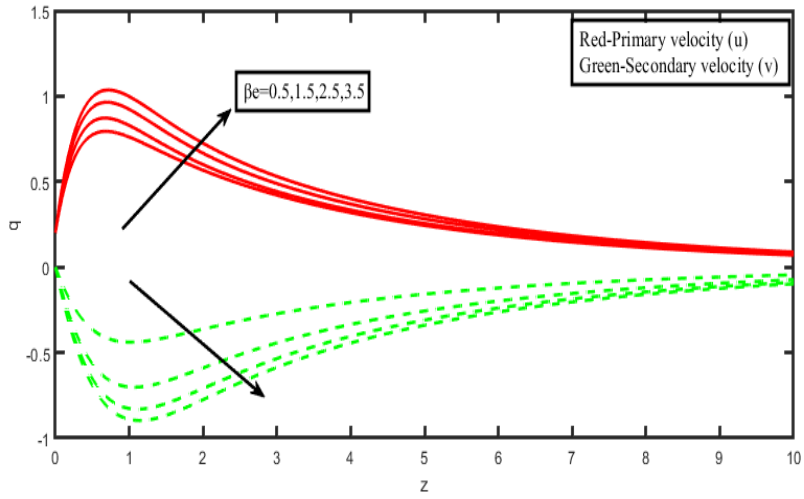

Figure 4. Velocity profiles for u and v for Hall parameter (β_e)

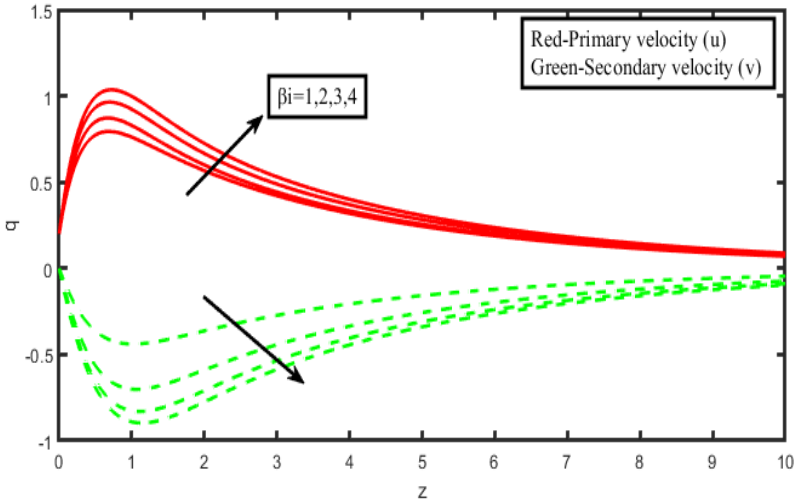

Figure 5. Velocity profiles for u and v for Hall parameter (β_i)

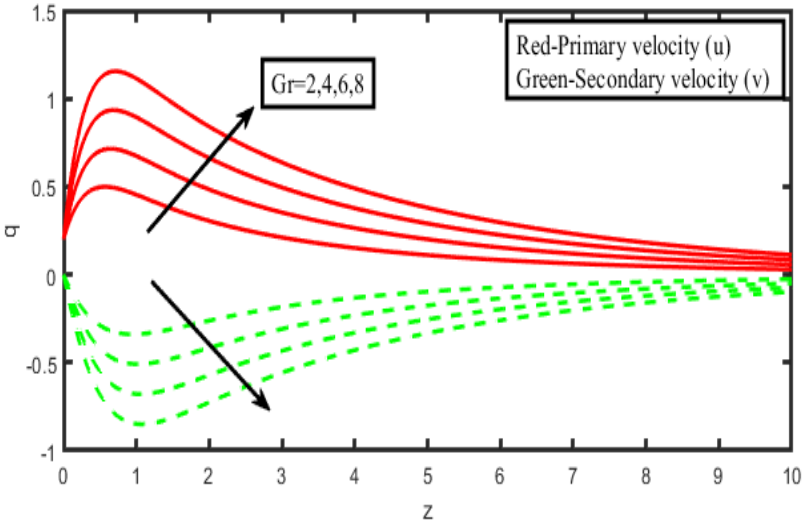

Figure 6. Velocity profiles for u and v for thermal Grashof number (Gr)

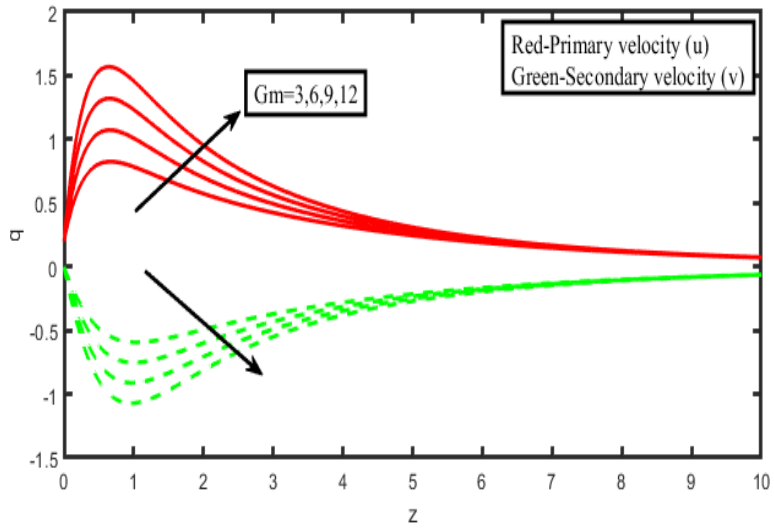

Figure 7. Velocity profiles for u and v for modified Grash of number (Gm)

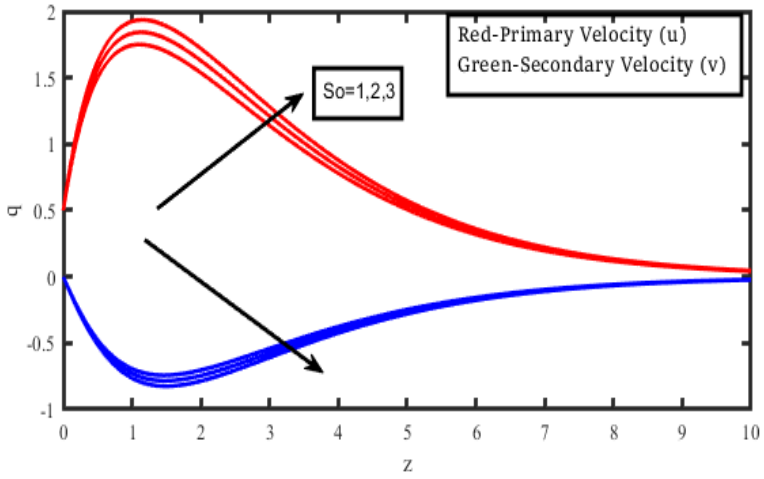

Figure 8. Velocity profiles for u and v for Soret Parameter (So)

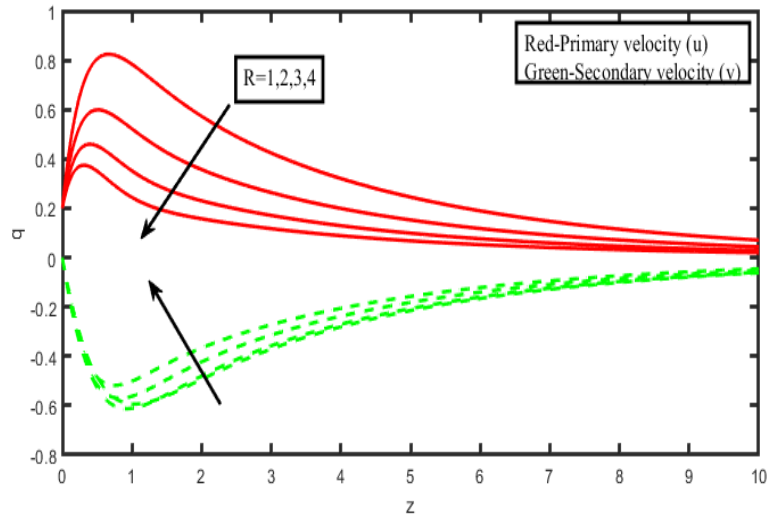

Figure 9. Velocity profiles for u and v for Rotation specification (R)

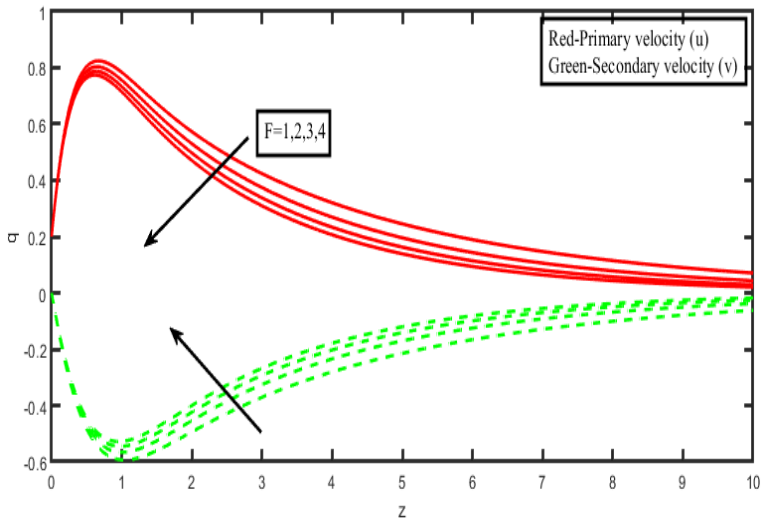

Figure 10. Velocity profiles for u and v for radiation parameter (F)

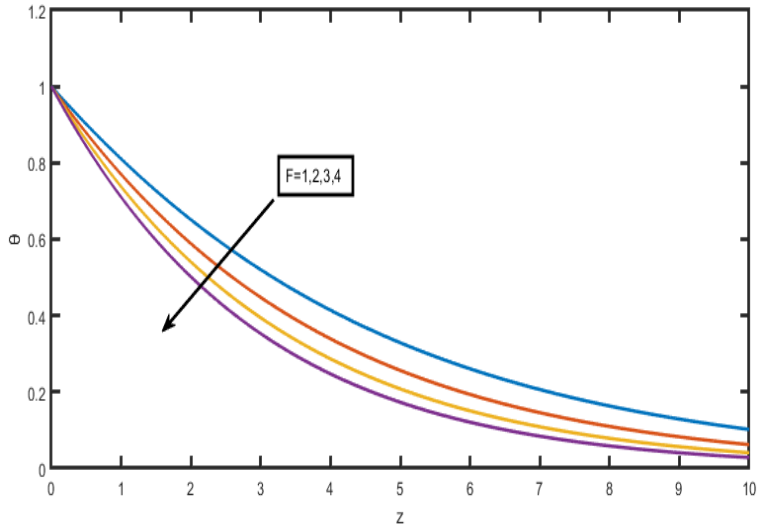

Figure 11. Temperature profiles for radiation parameter (F)

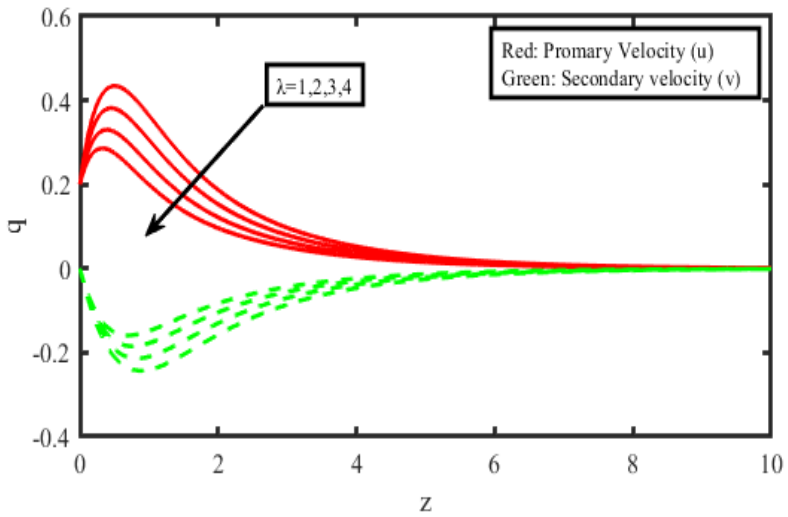

Figure 12. Velocity profiles for u and v for Jeffrey fluid parameter (λ)

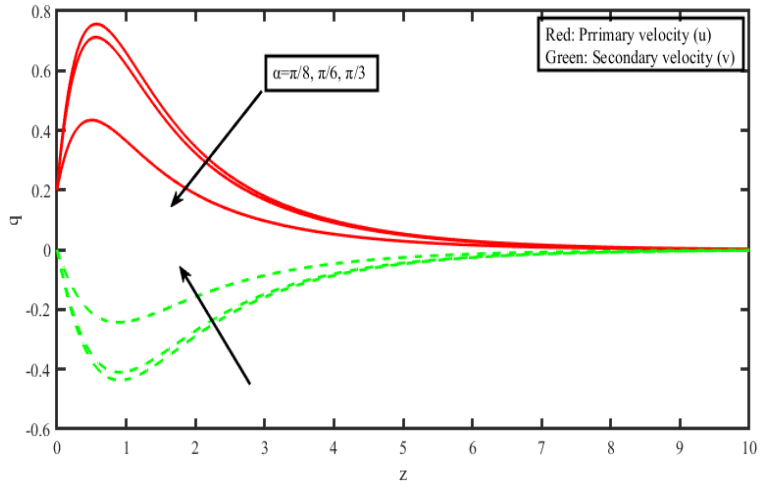

Figure 13. Velocity profiles for u and v for inclined parameter (α)

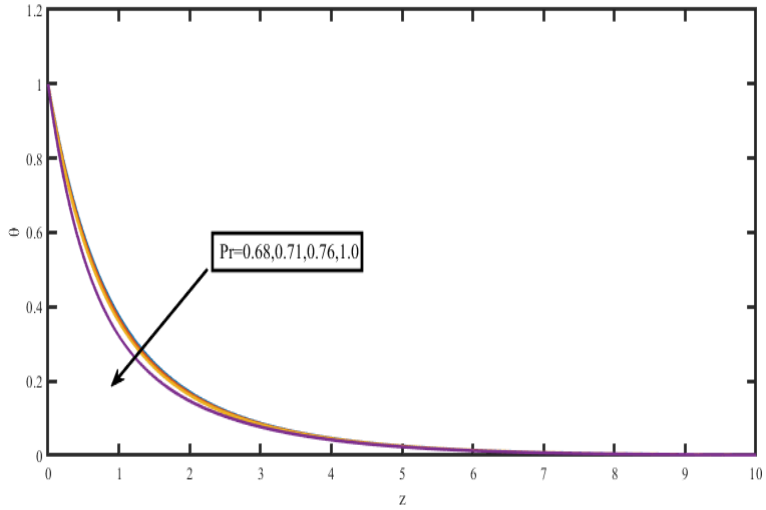

Figure 14. Temperature profiles for Prandtl number (Pr)

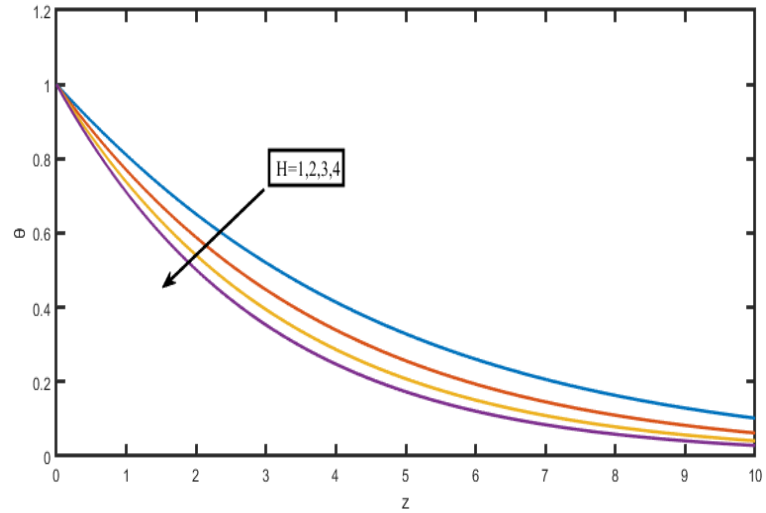

Figure 15. Temperature profiles for Heat absorption Parameter (H)

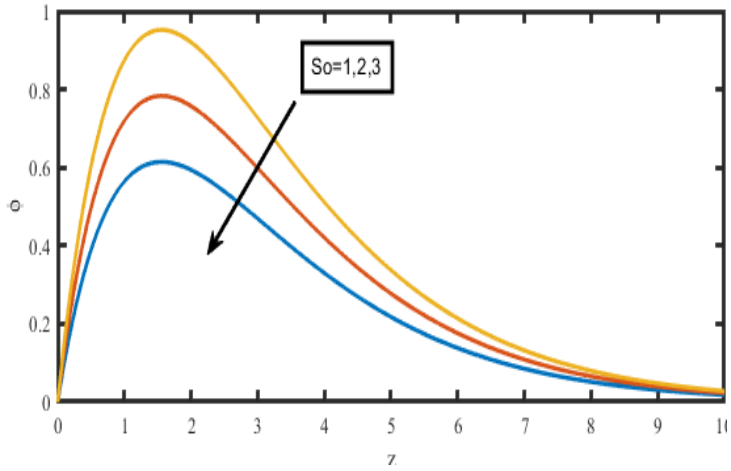

Figure 16: Concentration profiles for Soret Parameter (So)

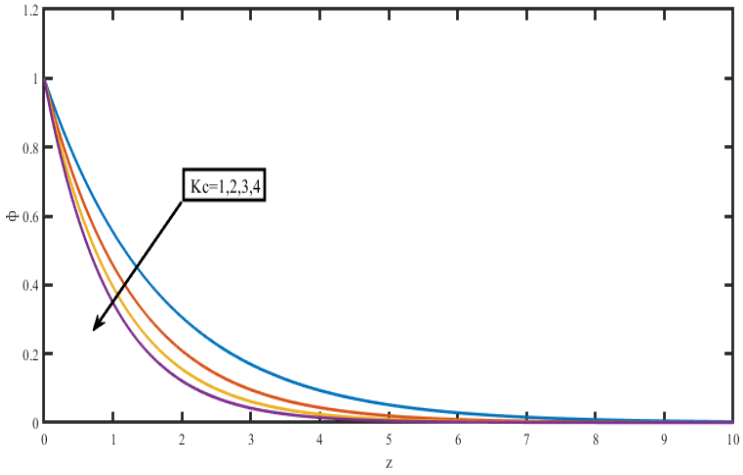

Figure 17. Concentration profiles for Chemical reaction (K_c)

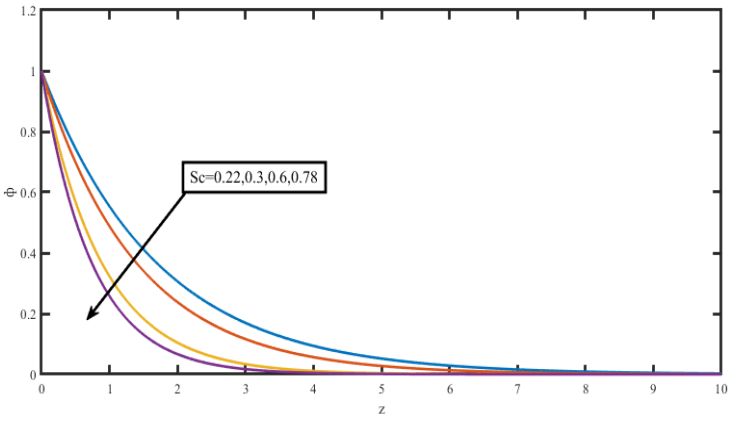

Figure 18. Concentration profiles for Schmidt number (Sc)

The magnitudes of skin friction are shown in the following table 1. An increase in the Hartmann number will be implemented to reduce skin friction. Because the elastic property of visco-elastic second-grade fluid minimized the frictional drag, it is used in this application. The effect of increasing the rotation parameter, the Prandtl number, the heat source parameter, the Schmidt number, the chemical reaction parameter, and the time on similar behavior is investigated. The expansion of skin friction in magnitude on the boundary of the surface

is further enhanced by an increase in the permeability parameter or second-grade fluid parameter, and the analogous behavior is examined for the same when an increase in thermal Grashof number, mass Grashof number, Hall and ion slip parameters are increased on the boundary of the surface. As a result, an increase in the radiation parameter, the Prandtl number, and the heat source parameters increase the Nusselt number, as shown in Table 2. It is lessened by increasing the heat source parameter and Prandtl number, and it has enhanced with increasing radiation parameter. According to Table 3, increasing the Schmidt number, chemical reaction and Soret parameters all lead to strengthening the Sherwood number as time progresses.

Table 1: Skin friction

M	**K**	**So**	**λ**	**Gr**	**Gm**	βe	βi	**Pr**	**H**	**R**	α	τ
2	0.5	0.5	0.5	5	3	1	0.2	0.71	1	1	π/3	2.3578
3	0.5	1	0.5	5	3	1	0.2	0.71	1	1	π/3	2.2345
2	0.5	2	0.5	5	3	1	0.2	0.71	1	1	π/3	3.1547
2	0.5	3	1.0	5	3	1	0.2	0.71	1	1	π/3	2.1258
2	0.5	1	1.5	5	3	1	0.2	0.71	1	1	π/3	2.4748
2	0.5	1	0.5	9	3	1	0.2	0.71	1	1	π/3	3.6878
2	0.5	1	0.5	12	3	1	0.2	0.71	1	1	π/3	2.6878
2	0.5	1	0.5	5	6	1	0.2	0.71	1	1	π/3	5.7015
2	0.5	1	0.5	5	9	1	0.2	0.71	1	1	π/3	3.0878
2	0.5	1	05	5	3	2	0.2	0.71	1	1	π/3	3.5785
2	0.5	1	0.5	5	3	3	0.2	0.71	1	1	π/3	4.5878
2	0.5	1	0.5	5	3	1	0.4	0.71	1	1	π/3	2.0024
2	0.5	1	0.5	5	3	1	0.6	0.71	1	1	π/3	3.1478
2	0.5	1	0.5	5	3	1	0.2	5.0	1	1	π/3	3.6587
2	0.5	1	05	5	3	1	0.2	7.0	1	1	π/3	2.8550
2	0.5	1	0.5	5	3	1	0.2	0.71	1	2	π/3	2.5478

Table 2. Nusselt number

F	**So**	**H**	**Pr**	ω	Nu
2	0.5	1	0.71	π/6	1.2875
3	0.5	1	0.71	π/6	1.5851
1	0.5	1	0.71	π/6	1.4983
1	0.5	2	0.71	π/6	1.3478
1	0.5	1	0.71	π/4	1.5789
1	0.5	1	7.0	π/3	1.5452

Table 3. Sherwood number

Sc	**Kc**	So	Sh
0.3	1	1	0.5854
0.6	1	1	0.7135
0.22	2	1	0.1290
0.22	3	1	0.7878
0.22	1	2	0.9887
0.22	1	3	1.5571

Table 4. Comparison of results for primary velocity (A= 5, n= 0.5, t= 0.5, ϵ= 0.01, U_0 = 0.5, m= 0, Sc= 0.22, Kc= H= So= 1)

M	K	Gr	Gm	Previous results Krishna et al [26]	Present values
2	0.5	5	3	0.703601	0.703484
3	0.5	5	3	0.452225	0.452455
4	0.5	5	3	0.302104	0.302545
2	1.0	5	3	0.795586	0.797822
2	1.5	5	3	0.832564	0.835478
2	0.5	10	3	0.932386	0.934587
2	0.5	15	3	1.166330	1.161458
2	0.5	5	6	0.780633	0.780458
2	0.5	5	9	0.85762	0.851458

CONCLUSIONS

Hall and ion-slip parameters tend to accelerate secondary fluid velocity throughout the boundary layer region whereas it has a reverse effect on the primary fluid velocity throughout the boundary layer region. Rotation tends to accelerate secondary fluid velocity throughout the boundary layer region whereas it has a reverse effect on the primary fluid velocity throughout the boundary layer region. Thermal buoyancy force tends to retard the secondary fluid velocity throughout the boundary layer region. Thermal buoyancy force tends to accelerate primary fluid velocity in the region near to the plate whereas it has a reverse effect on primary fluid velocity in the region away from the plate. Concentration buoyancy force tends to accelerate both the primary and secondary fluid velocities throughout the boundary layer region whereas mass diffusion has reverse effect on it throughout the boundary layer region. Permeability of the porous medium tends to accelerate the secondary fluid velocity throughout the boundary layer region whereas it has reverse effect on primary fluid velocity throughout the boundary layer region. The same behavior has observed in the case of Jeffrey fluid parameter and angle of inclination. Thermal and mass diffusion tends to retard species concentration and there is an enhancement in species concentration due to increasing Soret number and time throughout the boundary layer region. Thermal radiation tends to reduced rate of heat transfer whereas as chemical reaction, Heat source, and Prandtl number progress the rate of heat transfer is getting enhanced. Chemical reaction, Schmidt number and time tend to enhance the rate of mass transfer whereas thermal radiation and Soret number have reverse effect on it.

REFERENCES

[1] M.M. Bhatti, M.A. Abbas, "Simultaneous effects of slip and MHD on peristaltic blood flow of Jeffrey fluid model through a porous medium", Alexandr Eng J., Vol. 55, Pp. 1017-1023, 2016.

[2] P.B.A. Reddy, "Magnetohydrodynamic flow of a Casson fluid over an exponentially inclined permeable stretching surface with thermal radiation and chemical reaction", Ain Shams Eng J., Vol. 7, Pp. 593-602, 2016.

[3] M.K. Murthy, "Couette Flow of Jeffrey fluid in a porous channel with heat source and chemical reaction", Middle East J. Scient Res., Vol. 24, Pp. 585-592, 2016.

[4] N.S. Akbar, Z.H. Khan, S. Nadeem, "Influence of magnetic field and slip-on Jeffrey fluid in a ciliated symmetric channel with metachronal wave pattern", J. Appl Fluid Mech., Vol. 9, Pp. 565-572, 2016.

[5] N. Sandeep, C. Sulochana, "Momentum and heat transfer behaviour of Jeffrey, Maxwell and Oldroyd-B nanofluids past a stretching surface with non-uniform heat source/sink", Ain Shams Eng J., Vol. 9, No. 4, Pp. 517-524, 2018.

[6] N. Sandeep, C. Sulochana, I.L. Animasaun, "Stagnation-point flow of a Jeffrey nano fluid over a stretching surface with induced magnetic field and chemical reaction", Int. J. Eng Resaech in Afrika, Vol. 20, Pp. 93-111, 2016.

[7] N. Sandeep, "Effect of aligned magnetic field on liquid thin film flow of magnetic- nanofluid embedded with graphene nanoparticles", Adv Powder Technol., Vol. 28, Pp. 865-875, 2017.

[8] M.A. Samad, M. Mansur-Rahman, "Thermal radiation interaction with unsteady MHD flow past a vertical porous plate immersed in a porous medium", J. Naval Architect. Marine Eng., Vol. 3, No. 1, Pp. 7–14, 2006.

[9] S. Sangapatnam, R.B. Nandanoor, P.R. Vallampati, "Radiation and mass transfer effects on MHD free convection flow past an impulsively started isothermal vertical plate with dissipation", Thermal Sci., Vol. 13, No. 2, Pp. 171–181, 2009.

[10] P.K. Kythe, P. Puri, "Unsteady MHD free convection flows on a porous plate with time-dependent heating in a rotating medium", Astrophys Space Sci., Vol. 143, No. 1, Pp. 51–62, 1988.

[11] J.N. Tokis, "Free convection and mass transfer effects on the magnetohydrodynamic flows near a moving plate in a rotating medium", Astrophys Space Sci., Vol. 144, No. 1–2, Pp. 291–301, 1988.

[12] N. Nanousis, "Thermal diffusion effects on MHD free convective and mass transfer flow past a moving infinite vertical plate in a rotating fluid", Astrophys Space Sci., Vol. 191, No. 2, Pp. 313–22, 1992.

[13] A.K. Singh, N.P. Singh, U. Singh, H. Singh, "Convective flow past an accelerated porous plate in rotating system in presence of magnetic field", Int J. Heat Mass Transfer., Vol. 52, No. 13–14, Pp. 3390–3395, 2009.

[14] V. M. Durga Prasad, S.S.K. Kumar, and S.V.K. Varma, "Heat and mass transfer analysis for the MHD flow of nanofluid with radiation absorption", Ain Shams Engineering Journal, Vol. 9, Pp. 801-813, 2018. 10.1016/j.asej.2016.04.016.

[15] S.P. Samrat, C. Sulochana, G.P. Ashwinkumar, "Impact of Thermal Radiation on an Unsteady Casson Nanofluid Flow over a Stretching Surface", Int. J. Appl. Comput. Math., Vol. 5, Pp. 31, 2019. https://doi.org/10.1007/s40819-019-0606-2

[16] K. Raghunath, G. Nagesh, V.R.C. Reddy, M. Obulesu, "Unsteady MHD fluid flow past an inclined vertical porous plate in the presence of chemical reaction with aligned magnetic field, radiation, and Soret effects", Heat Transfer., Vol. 51, Pp. 1-19, 2021. DOI: 10.1002/htj.22423.

[17] R. Kodi, O. Mopuri, "Unsteady MHD oscillatory Casson fluid flow past an inclined vertical porous plate in the presence of chemical reaction with heat absorption and Soret effects", Heat Transfer, Vol. 51, No. 3, Pp. 1-19, 2021. DOI: 10.1002/htj.22327

[18] R. Kodi, O. Mopuri, S. Sree, V. Konduru, "Investigation of MHD Casson fluid flow past a vertical porous plate under the influence of thermal diffusion and chemical reaction", Heat Transfer, Vol. 51, No. 3, Pp. 77–394, 2021. DOI: 10.1002/htj.22311

[19] R.R. Vaddemani, R. Kodi, O. Mopuri, "Characteristics of MHD Casson fluid past an inclined vertical porous plate", Materials Today: Proceedings, Vol. 49, Pp. 2136–2142, 2022. https://doi.org/10.1016/j.matpr.2021.08.328.

[20] A. Raptis, C.V. Massalas, "Magnetohydrodynamic flow past a plate by the presence of radiation", Heat Mass Transfer, Vol. 34, No. 2– 3, Pp. 107–109, 1998.

[21] A.J. Chamkha, "Thermal radiation and buoyancy effects on hydromagnetic flow over an accelerating permeable surface with heat source or sink", Int J. Eng Sci., Vol. 38, No. 15, Pp. 1699–712, 2000.

[22] C.I. Cookey, A. Ogulu, V.B. Omubo-Pepple, "Influence of viscous dissipation and radiation on unsteady MHD free convection flow past an infinite heated vertical plate in a porous medium with time-dependent suction", Int J. Heat Mass Transfer, Vol. 46, No. 13, Pp. 2305–11, 2003.

[23] S. Suneetha, R.N. Bhaskar, P.V. Ramachandra, "Thermal radiation effects on MHD free convection flow past an impulsively started vertical plate with variable surface temperature and concentration". J. Naval Arch Marine Eng., Vol. 5, No. 2, Pp. 57–70, 2008.

[24] A. Ogulu, O.D. Makinde, "Unsteady hydromagnetic free convection flow of a dissipative and radiating fluid past a vertical plate with constant heat flux", Chem. Eng. Commun., Vol. 196, No. 4, Pp. 454–62, 2008.

[25] M.A.A. Mahmoud, "Thermal radiation effect on unsteady MHD free convection flow past a vertical plate with temperature dependent viscosity", Can. J. Chem. Eng., Vol. 87, No. 1, Pp. 47–52, 2009.

[26] M.V. Krishna, A.J. Chamkha, "Hall and ion slip effects on MHD rotating flow of elastico-viscous fluid through porous medium", Int. Commun. Heat Mass Transfer., Vol. 113, Pp. 104494, 2020, 10.1016/j.icheatmasstransfer.2020.104494

[27] M.V. Krishna, "Hall and ion slip effects on MHD free convective rotating flow bounded by the semi-infinite vertical porous surface", Heat Transfer, Vol. 49, No. 4, pp. 1920-1938, 2020. 10.1002/htj.21700

[28] M.V. Krishna, "Hall and ion slip effects on MHD laminar flow of an elastic-viscous (Walter's-B) fluid", Heat Transfer, Vol. 49, No. 4, Pp. 2311-2329, 2020. https://doi.org/10.1002/htj.21722

[29] M.V. Krishna, K. Jyothi, A.J. Chamkha, "Heat and mass transfer on unsteady, magnetohydrodynamic, oscillatory flow of second-grade fluid through a porous medium between two vertical plates, under the influence of fluctuating heat source/sink, and chemical reaction", Int. Jour. of Fluid Mech. Res., Vol. 45, No. 5, Pp. 459-477, 2018. 10.1615/InterJFluidMechRes.2018024591

[30] K.P. Cramer, S.I. Pai, "Magneto Fluid Dynamics for Engineers and Applied Physics", McGraw-Hill Book Co, New York, 1973.

[31] G. Grief, I.S. Habib, L.C. Lin, "Laminar convection of a radiating gas in a vertical channel", J. Fluid Mech., Vol. 45, Pp. 513–520, 1971.

[32] G. Sutton, A. Sherman, "Engineering Magnetohydrodynamics", Mc Graw Hill, New York, 1965.